Instability Induced by Dry Friction

Domenico Guida, Fabio Nilvetti, and Carmine Maria Pappalardo

***Abstract*—A theoretical analysis of the dynamic behavior of mechanical systems characterized by coupled e-lements subjected to friction force from the sliding surface is proposed. With reference to systems with one degree of freedom, and approximating the friction force as a piecewise linear function, i.e. straight line segments with a suitable slope, the positioning errors in the stop phase are studied. Dimensionless analytical relations used to predict the size of positioning errors and dimensionless diagrams are provided. Furthermore the influence of the dry friction on the dynamics of a system with two degrees of freedom is proposed. The model system consists of a body of mass m_1, constrained by means of a spring and a damper to a driving support, moving relatively to its counterpart of mass m_2. In the conditions stability of the position of equilibrium vibrations due the static friction and the support's velocity have been pointed out.**

***Index Terms*—Self Excited Vibrations, Dry Friction, Friction Instability, Limit Cycle, Stick-Slip.**

I. Introduction

THE dynamic behavior of many tribomechanical systems is influenced by the interfacial friction processes between the moving components: in particular, self-excited vibrations or positioning errors in the stop phase of the controlled body can arise in certain operating conditions.

In this connection it is well known that stick-slip phenomena can arise in the moving parts of relative motion machines, particularly in dry or limit friction conditions.

This phenomenon consists of typical vibrations, characterized by a phase of uniform motion (stick) followed by a phase of non-uniform motion (slip), which can be caused when there is a considerable difference between the static and the kinetic friction coefficients and, more generally, when a non-linear friction-velocity characteristic occurs [16] and [17].

The negative effects deriving from this are principally severe wear of the mechanical components and undesirable fatigue and noise which can thus compromise system operation.

In previous papers [18], [19], [20] tribomechanical systems with one degree of freedom were modeled in a simplified manner with reference to a slide-spring-damper system.

The friction-speed force characteristic was approximated using appropriate piecewise linear functions, i.e. straight line segments with a suitable slope, and a discontinuity at a null value of the relative speed. The use of analytical methods in analyzing stick-slip instability conditions made it possible to build straightforward stability maps that allow predictions to be made on the occurrence of self-excited vibrations, once the system parameters have been assigned, and to optimize the choice of parameters in the design phase.

One way of preventing the occurrence of stick-slip self-excited vibrations is to introduce viscous dampers so as to vary the slopes of the sections approximating the friction-speed characteristic. However, this solution can give rise to an equally undesirable effect as it may entail slide positioning errors in the stop phase.

This problem is of particular importance in robot members, in automatic regulation systems, in hydraulic systems and in the slides of machine tools where ”jumps” may occur, sometimes measuring a few millimeters. Such jumps may cause the piece being machined to take up a position different from the programmed one, thus compromising the accuracy and precision of the machine process. This situation assumes even more serious proportions in numeric control machine tools. Hence we can see that a correct analysis of the dynamic behavior of a tribomechanical system cannot be limited to studying slide stability in relative motion conditions, but must necessarily be extended to include the system stop phase.

The present paper build on a previous study [21] and summarizes the main results obtained [20], which allow the occurrence of stick-slip vibrations to be prevented.

The paper then goes on to determine the slide positioning error in the drive mechanism stop phase, approximating the friction characteristic with a piecewise linear function with a discontinuity at the relative speed null value, and assuming that the static friction is greater than the kinetic friction when assessed in incipient motion conditions.

Substitution of the variable in the motion equation then gives a first order differential equation governing system evolution in the phase plane. Once the system's characteristic parameters are known, the proposed analysis makes it possible to obtain results of immediate utility through dimensionless analytical relations and in the form of operative diagrams.
Finally, in the paper is described dry friction influence upon the dynamic behavior of a two degrees of freedom composed of a body of mass m_1, constrained by means of a spring and a damper to a driving support, moving relatively to its counterpart of mass m_2.

II. System Dynamic Behavior

The determination of the positioning error that the slide in Figure 1 may present in the drive mechanism stop phase assumes meaning, as will be shown in the following sections, only when the system is stable in terms of stick-slip vibrations.

Analysis of stick-slip instability is thus a preliminary step and has been tackled in previous papers [18], [19] and [20]. It is nevertheless here considered necessary to take up the same basic approach and provide application results that

D. Guida is with the Department of mechanical Engineering, University of Salerno, Fisciano, SA, 84084 ITALY (e-mail: guida@unisa.it).

F. Nilvetti is with the Department of mechanical Engineering, University of Salerno, Fisciano, SA, 84084 ITALY (e-mail: fnilvetti@unisa.it).

C. M. Pappalardo is with the Department of mechanical Engineering, University of Salerno, Fisciano, SA, 84084 ITALY (e-mail: cpappalardo@unisa.it).

make it possible to exclude self-excited vibrations, once the characteristic parameters of the system in question are known.

A. Stick-Slip Instability

Analysis of the dynamic behavior of the system in Figure 1 was performed assuming that the force F contain the viscous damping force F_σ as well as the friction force F_a between the slide and the sliding surface, considering that the drive mechanism speed is constant. Assuming that the friction force can be approximated with a piecewise linear function (Fig. 2) and putting:

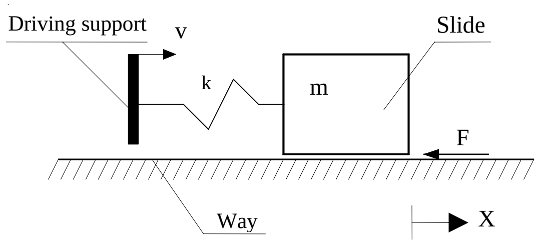

Fig. 1. The physical system

$$
\begin{array}{lll}
\bar{x} = X(t) - vt; & \omega_n^2 = \frac{k}{m}; & x = \frac{\bar{x}}{v}\omega_n; \\
\sigma = \bar{\sigma}\sigma_c; & \sigma_c = 2\sqrt{km}; & \tau = \omega_n t; \\
f_1(\dot{x}+1) = \frac{1}{m\omega_n v}F; & p_1 = -\frac{v^*}{v}; & p_2 = \frac{v^*-v}{v^*} \\
p^* = \frac{p_1}{p_2}; & (\dot{\cdot}) = \frac{d}{d\tau}; &
\end{array}
\tag{1}
$$

the force F can be represented in the dimensionless form shown in Figure 3 , and assumes the form:

$$
f_1(\dot{x}+1) =
$$

$$
= \begin{cases}
f_{1c} + 2\mu_1(1+\dot{x}), & -1 < \dot{x} \le p^* \\
f_{1c} + 2\mu_2(1+\dot{x}) + \\
\quad +2(\mu_1-\mu_2)(1+p^*), & \dot{x} \ge p^* \\
f_{1s}, & \dot{x} = -1^+ \\
f'_{1s}, & \dot{x} = -1^- \\
f'_{1c} + 2\mu_1(1+\dot{x}), & -(2+p^*) \le \dot{x} < -1 \\
f'_{1c} + 2\mu_2(1+\dot{x}) + \\
\quad +2(\mu_1-\mu_2)(1+p^*), & \dot{x} \le -(2+p^*)
\end{cases}
\tag{2}
$$

where, with the relations in figures 2 and 3 :

$$
\begin{array}{ll}
f_{1s} = f_{as} - 2\sigma & \varepsilon = f_s - f_c = \frac{F_{as}-F_{ac}}{m\omega_n v^*} \\
f'_{1s} = -f_{as} - 2\sigma & 2\mu_1 = \tan\alpha_1 + 2\sigma \\
f_{1c} = f_{ac} - 2\sigma & 2\mu_2 = \tan\alpha_2 + 2\sigma \\
f'_{1c} = -f_{ac} - 2\sigma & \mu_3 = \mu_1 \\
F_{as} = (m\omega_n v)\, f_{as} & \mu_4 = \mu_2 \\
F_{ac} = (m\omega_n v)\, f_{ac} &
\end{array}
\tag{3}
$$

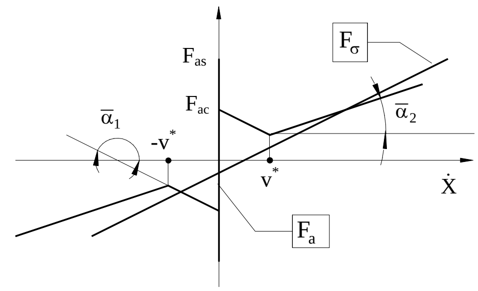

Fig. 2. Friction characteristic and viscous damping force vs. relative sliding velocity

Assuming a system of coordinates fixed O-X in the slide plane and taking into account positions (1) and (2), the following dimensionless motion equation can be obtained:

$$
\ddot{\mathrm{x}} + \mathrm{f}_1(\dot{\mathrm{x}}+1) + \mathrm{x} = 0 \tag{4}
$$

Substituting the variable $x = p(\dot{x})$ in (3) gives a first order differential equation that must satisfy the evolution of the system in the phase plane. Analytical integration of the above differential equation can now take place, imposing conditions of phase trajectory continuity at the angular points of the friction characteristic and considering that the relative speed of the slide compared to the plane is null in the stick phase. It is thus possible to identify the set of parameters that determine the system's critical stability conditions [19] and [20].

This analysis made it possible to identify the parametric space regions corresponding to self-excited, friction-caused vibrations (Fig. 4), i.e. to build stability maps (Figs. 5) that enable predictions to be made on the occurrence of stick-slip vibrations once system parameters have been as-signed. The domain below every surface (curves of Figure 4) identifies the values of ϵ , μ_1 and μ_2 (ϵ , μ_2; $p^* = cost$) that cause undesirable self-excited stick-slip oscillations.

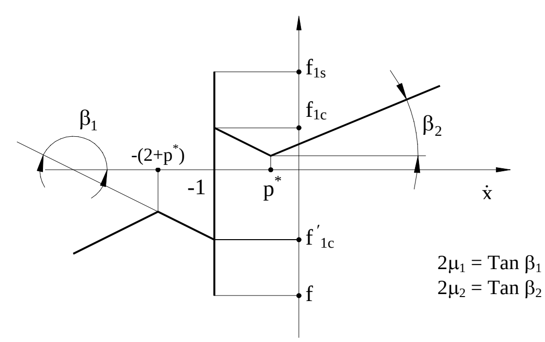

Fig. 3. Dimensionless friction-velocity characteristic

B. Analysis of positioning errors in the stop phase

In the drive mechanism stop phase, the dynamic behavior of the system is analyzed under the assumption of a system of coordinates O-X fixed in the guide plane and assuming a friction characteristic of the type shown in Figures 2 and 3. The slide motion equation is:

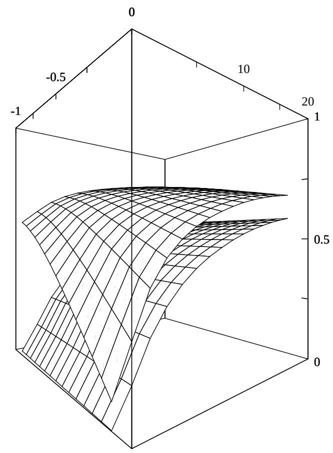

Fig. 4. Stability map for p* = -0.1 and p* = -0.9

$$m\ddot{x} + F\left(\dot{x}\right) + k\left(x - vt\right) = 0 \tag{5}$$

which with the positions:

$$x = \frac{\bar{x}}{v^*}\omega_n; \qquad f = \frac{1}{m\omega_n v^*}F \tag{6}$$

can be rewritten in the following dimensionless form:

$$\ddot{x} + f\left(\dot{x} - p_1\right) + x = 0 \tag{7}$$

The meaning of parameters p_1 and p_2 can be deduced by analyzing the dimensionless friction-velocity characteristic illustrated in Figure 4 and is defined by the following relation (8):

$$f(\dot{x} - p_1) =$$

$$= \begin{cases} f_c + 2\mu_1(\dot{x} - p_1), & p_1 < \dot{x} \le p_2 \\ f_c + 2(\mu_1 - \mu_2)+ \\ \quad +2\mu_2(\dot{x} - p_1), & \dot{x} \ge p_2 \\ f_s, & \dot{x} = p_1^+ \\ f_s', & \dot{x} = p_1^- \\ f_c' + 2\mu_1(\dot{x} - p_1), & -(2 - p_2) \le \dot{x} < -p_1 \\ f_c' + 2(\mu_1 - \mu_2)+ \\ \quad +2\mu_2(\dot{x} - p_1), & \dot{x} \le -(2 - p_2) \end{cases} \tag{8}$$

where:

$$\begin{array}{l} f_c = f_{ac} + 2p_1\sigma \\ f_s = f_{as} + 2p_1\sigma \\ f_c' = -f_{ac} + 2p_1\sigma \\ f_s' = -f_{as} + 2p_1\sigma \end{array} \tag{9}$$

With reference to two friction forces characterized by different slopes μ_2 (Fig. 7) the point E defined by the intersection of

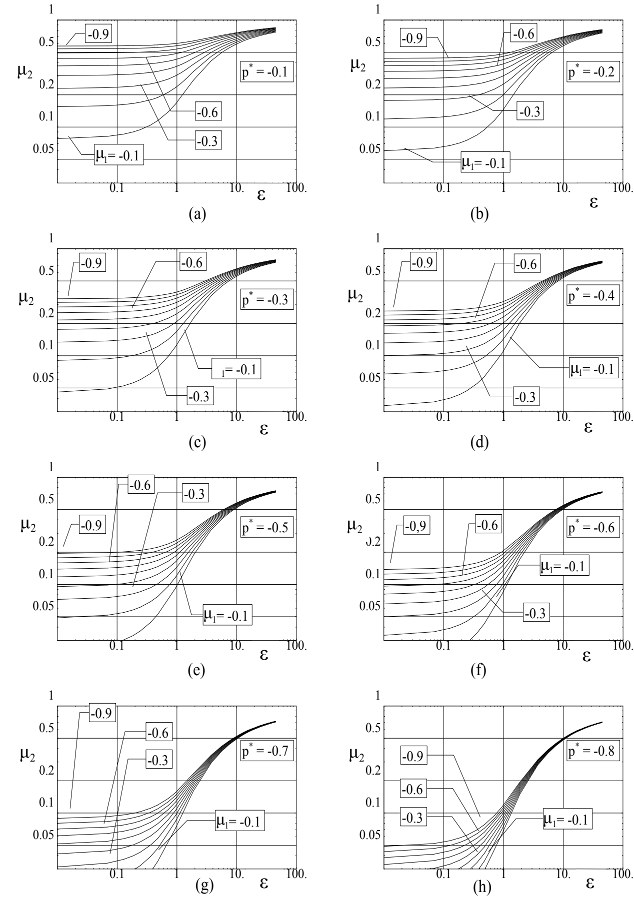

Fig. 5. Limit stability curves for: p*= -0.1 (a), p*= -0.2 (b), p* = -0.3 (c), p* = -0.4 (d), p* = -0.5 (e), p* = -0.6 (f), p* = -0.7 (g), p* = -0.8 (h)

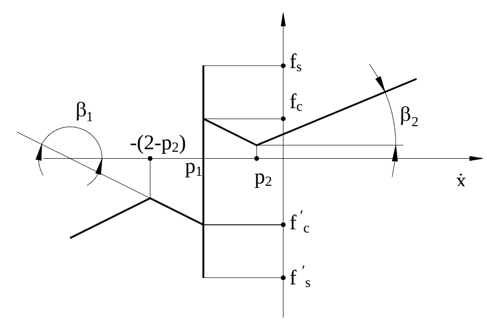

Fig. 6. Dimensionless friction-velocity characteristic

the curve $x = -f(\dot{x} - p_1)$ where the abscissa axis represents the slide's stationary equilibrium position when the system mechanism is moved at a constant speed. Because of the assumptions made, this equilibrium position is asymptotically stable.

In the stop phase the system can display two different dynamic behaviors which are qualitatively illustrated in Figures 7 and 8. A friction characteristic such as the one in Figure 7 does not entail position errors in the stop phase. For null drive mechanism speeds, point E is always an equilibrium.

Whereas positioning errors in the drive mechanism stop phase occur when the friction characteristic is of the type shown in Figure 8. In this case, point E no longer represents the slide's equilibrium position and so the system evolves in accordance with a phase trajectory of the type shown in Figure 8 where the resulting positioning error is also indicated.

In general terms, the system can evolve according to three different trajectories, which are illustrated in Figure 9: a curve of type "a" is found when the point of equilibrium is such that the phase trajectory does not intersect the straight line $x = 1$. More specifically, this situation arises when, for a given slope μ_1, point E is located to the right of point E^*, which is the intersection with the x axis of the particular phase trajectory that is tangential to the straight line $x = 1$.

Trajectories of types "b" and "c" are en countered when, for the same μ_1 slope value, point E lies to the left of point E^*, and the slope μ_2 is greater than 1 or between 0 and 1 respectively. Indicating with $x(t^*)$ the position of the slide at

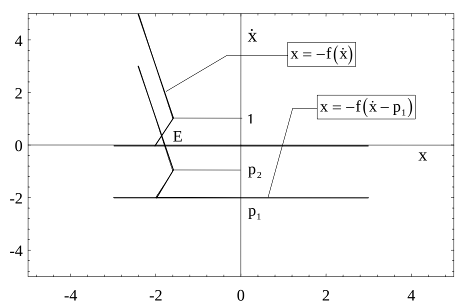

Fig. 7. Equilibrium point in the phase plain

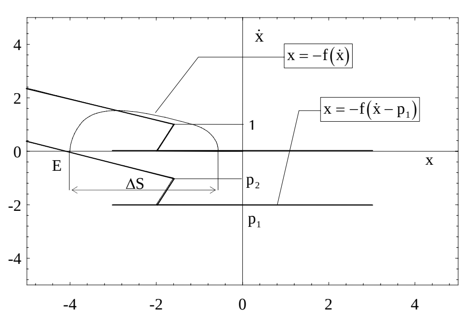

Fig. 8. Positioning error in the drive mechanism stop phase

the moment the drive mechanism stops, we may find that:

$$\begin{array}{l} x\left(t^*+\Delta t\right)-x\left(t^*\right)=0 \\ \text{or} \\ x\left(t^*+\Delta t\right)-x\left(t^*\right)\geq 0 \end{array} \tag{10}$$

Defining the slide positioning error in the dimensional and dimensionless form respectively with:

$$\Delta\bar{S} = x\left(t^*+\Delta t\right)-x\left(t^*\right) \tag{11}$$

and

$$\Delta S = \Delta\bar{S}\omega_n/v^* \tag{12}$$

for $\Delta S = 0$ to be true it is sufficient that the following relation holds:

$$F(\dot{x})_{\dot{x}=v} < F_s \tag{13}$$

which in dimensionless term is:

$$f\left(\dot{x}\right)_{\dot{x}=0} < f_s \qquad for \qquad x = 0 \tag{14}$$

In fact (Fig. 7) in system stop conditions, the discontinuity of the curve $x = -f(\dot{x})$ overlaps the abscissa axis of the phases plane. In this case all the points corresponding to the discontinuity are system equilibrium positions. In drive mechanism stop conditions, if Equation (14) is not true, the representation of the possible system dynamic evolutions in the phases plane is of the type shown in Figure 9. The error ΔS is determined by solving the following motion equation.

$$\ddot{x} + f(\dot{x}) + x = 0 \tag{15}$$

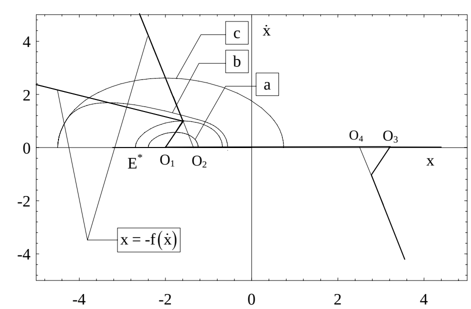

Fig. 9. Trend of trajectory in the drive mechanism stop phase

As the friction characteristic is a piecewise linear function of the speed, Equation (15) can be separated into four equations:

$$\begin{array}{ll} \ddot{x}_1 + f_1\left(\dot{x}_1\right) + x_1 = 0 & \dot{x} \geq 1 \\ \ddot{x}_2 + f_2\left(\dot{x}_2\right) + x_2 = 0 & 0 < \dot{x} < 1 \\ \ddot{x}_3 + f_3\left(\dot{x}_3\right) + x_3 = 0 & -1 < \dot{x} < 0 \\ \ddot{x}_4 + f_4\left(\dot{x}_4\right) + x_4 = 0 & \dot{x} \leq -1 \end{array} \tag{16}$$

where x_i indicates the relative shifts compared to the references originating in O_1, O_2, O_3 and O_4. The solutions of Equation (16) are of the type:

$$x_i = C\psi(u_i, \mu_i) \tag{17}$$

where $u = \dot{x}_i/x_i$ and C are used to indicate constant integration. The function $\psi\left(u_i, \mu_i\right)$ is

$$\begin{array}{l} \psi\left(u_i, \mu_i\right) = \frac{1}{\sqrt{u_i^2+2\mu_i u_i+1}} \cdot \\ \qquad \cdot \exp\left[\frac{\mu_i}{\sqrt{1-\mu_i^2}}\tan^{-1}\frac{u_i+\mu_i}{\sqrt{1-\mu_i^2}}\right] \qquad \left|\mu_1\right| < 1 \end{array} \tag{18}$$

If the phase trajectory is of type (a) or (b) in Figure 9, the error ΔS is determined by integrating the second of Equation (16) to obtain respectively:

$$\Delta S = (f(0) - f_c)\, e^{\frac{-\mu_1 \pi}{\sqrt{1-\mu_1^2}}}$$
$$\Delta S \cong (f(0) - f_c) + \frac{-2\mu_1}{\psi\left(-\frac{1}{2\mu_1}, \mu_1\right)} \tag{19}$$

Whereas, if the phase trajectory is of type (c) in Figure 9, in analogy with the method proposed by the authors in a previous paper [23], the error ΔS can be determined by imposing the continuity of the trajectory in points P_1, P_2 and P_3. In this way, the operative diagrams in Figures 10 and 11 can be built. The parameter $\lambda = f(0) - f_c + 2\mu_2$ is given on the abscissa axis and the quantity ΔS_λ on the ordinates axis. The positioning error in the drive mechanism stop phase is thus given by the relation:

$$\Delta S = \Delta S_\lambda + \lambda \tag{20}$$

Each diagram has been built by fixing the μ_1 slope value of the first section of the friction characteristic and assuming the slope μ_2 as the curve parameter. The diagrams in Figures 10 refer to values of the μ_1 parameter in the range $[0, -1]$. Whereas the diagrams in Figures 11 refer to values of μ_1 that are less than -1.

An analysis of Figures 10 makes it possible to point out that for μ_1 parameter values in the range $[0, -1]$ and values of the λ parameter less than the corresponding value E_1, the slope of the second section of the friction characteristic does not affect the positioning error in the stop phase. In general, as can be seen from Figures 10 and 11, the positioning error increases as the μ_1 parameter diminishes and increases as the μ_2 parameter increases.

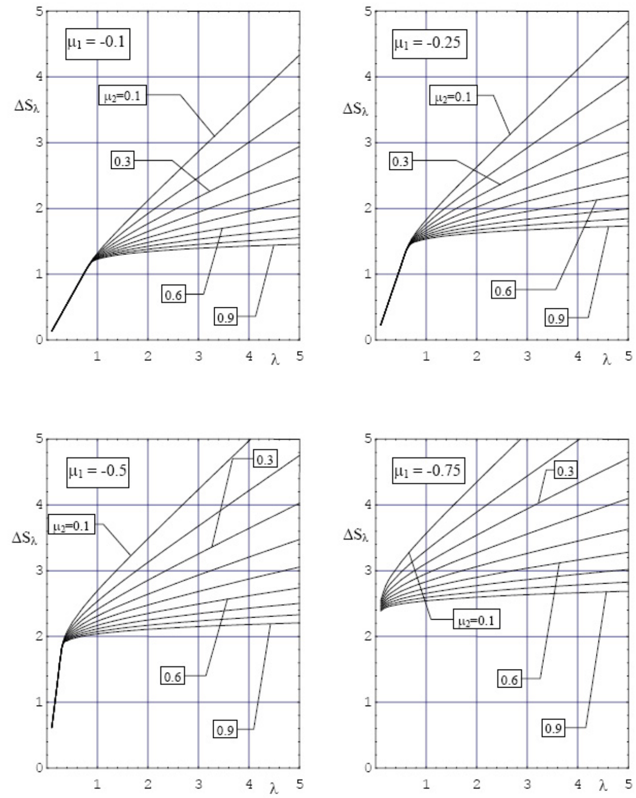

Fig. 10. Operative diagrams to predict the size of positioning errors for: $\mu_1 = -0.1$, $\mu_1 = -0.25$, $\mu_1 = -0.5$, $\mu_1 = -0.75$

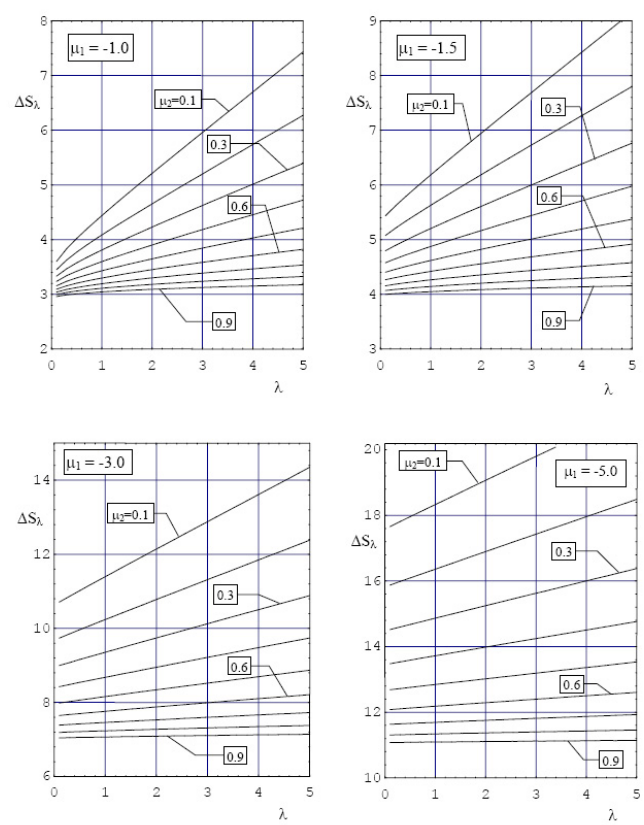

Fig. 11. Operative diagrams to predict the size of positioning errors for: $\mu_1 = -1.0$, $\mu_1 = -1.5$, $\mu_1 = -3.0$, $\mu_1 = -5.0$

III. Mathematical Model

Let X_1 and X_2, respectively, the displacement of the slides of mass m_1 and m_2 in the reference frame system indicated in Figure 12. The motion equations can be written so as indicated in the following relations:

$$\begin{cases} m_1\ddot{X}_1 + \sigma_1\left(\dot{X}_1 - v\right) + k_1\left(X_1 - vt\right) + \\ \qquad + F\left(\dot{X}_1 - \dot{X}_2\right) = 0 \\ m_2\ddot{X}_2 + \sigma_2\dot{X}_2 + k_2 X_2 - F\left(\dot{X}_1 - \dot{X}_2\right) = 0 \end{cases} \tag{21}$$

The friction characteristic is assumed to be piecewise linear function as shown in Figure 13. This function is analytically expressed by the followings relationships:

$$F\left(\dot{X}_1 - \dot{X}_2\right) = \begin{cases} F_c & \dot{X}_1 - \dot{X}_2 > 0 \\ F_s & \dot{X}_1 - \dot{X}_2 = 0^+ \\ F \quad |F| < F_s & \dot{X}_1 - \dot{X}_2 \equiv 0 \\ -F_s & \dot{X}_1 - \dot{X}_2 = 0^- \\ -F_c & \dot{X}_1 - \dot{X}_2 < 0 \end{cases} \tag{22}$$

Putting:

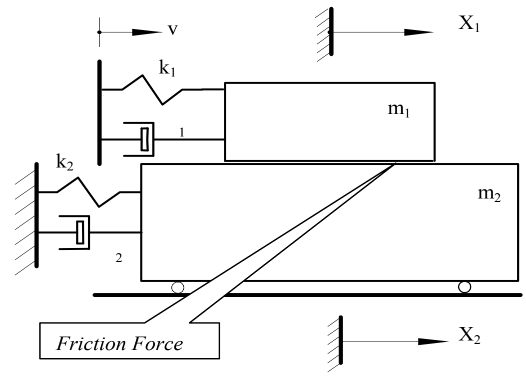

Fig. 12. System Model

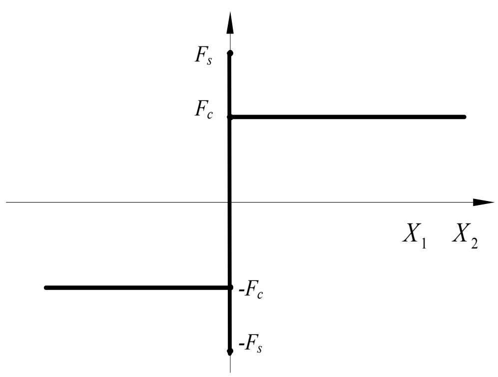

Fig. 13. Friction Force Characteristic

$$\begin{array}{lll} x_1 = X_1 - vt & \tau = \omega_1 t & \\ \mathrm{x}_2 = \mathrm{X}_2 & (\cdot) = d/d\tau & \\ \dfrac{\sigma_1}{m_1\omega_1} = 2s_1 & \dfrac{\sigma_2}{m_2\omega_2} = 2s_2 & \\ \dfrac{\mathrm{F_c}}{\mathrm{m_1}\omega_1 v} = f_{c1} & \dfrac{\mathrm{F_s}}{\mathrm{m_1}\omega_1 v} = f_{s1} & \\ \omega_1^2 = \dfrac{k_1}{m_1} & \omega_2^2 = \dfrac{k_2}{m_2} & \\ \dfrac{m_1}{m_2} = r & \dfrac{\omega_1}{\omega_2} = \zeta & \dfrac{\beta}{m_1\omega_1} = 2\mu_1 \\ \left(x_1\dfrac{\omega_1}{v}\right) = \eta_1(\tau) & \left(x_2\dfrac{\omega_1}{v}\right) = \eta_2(\tau) & \end{array} \tag{23}$$

the equations (23) can be rewritten as follows:

$$\begin{cases} \ddot{\eta}_1 + 2s_1\dot{\eta}_1 + \eta_1 + \\ \qquad + \dfrac{1}{m_1\omega_1 v}F\left\{v\left[(\dot{\eta}_1 - \dot{\eta}_2)\right] + 1\right\} = 0 \\ \ddot{\eta}_2 + 2s_2\dot{\eta}_2 + \dfrac{1}{\zeta^2}\eta_2 + \\ \qquad + \dfrac{r}{m_1\omega_1 v}F\left\{-v\left[(\dot{\eta}_1 - \dot{\eta}_2)\right] + 1\right\} = 0 \end{cases} \tag{24}$$

By the integration of the (24) it is possible to determine the dynamic behavior of the system for assigned initial conditions. The system (24) is a dynamical system with piecewise linear structure. Such systems, because of the friction force discontinuity, are difficult to be analyzed analytically and numerically. In this work we have debugged a numerical procedure that take advantage of the uncoupling of the motion equations in all the phases space points in which the following relationship isnt verified:

$$\dot{\eta}_1 - \dot{\eta}_2 = -1 \tag{25}$$

The system (24) exhibits only one equilibrium position and such solution results stable asymptotically. More exactly, the (24) close to the equilibrium position can be written in the following form:

$$\ddot{\eta} + B\dot{\eta} + K\eta = 0 \tag{26}$$

The system stability is verified if the symmetrical matrix K and the symmetrical part of the matrix B are defined positive [8]. Since the stability of the equilibrium position is verified for:

$$\left(s_1\frac{s_2}{r\zeta}\right)\left(s_1 + \frac{s_2}{r\zeta}\right)^{-1} > -\mu \tag{27}$$

where is the gradient of the friction characteristic in the equilibrium position [7] and the other parameters are indicated in the relations (23). In the case in matter the (27) is always verified since there is no gradient of the friction characteristic. It comes out obvious that for zero support speed, the system will exhibit infinity of equilibrium position to which will tend, in an finite time.

In Figure 14 the dynamic behavior of the system is shown. Such system does not exhibit limit cycles, or rather it does not show vibrations for any initial conditions set.

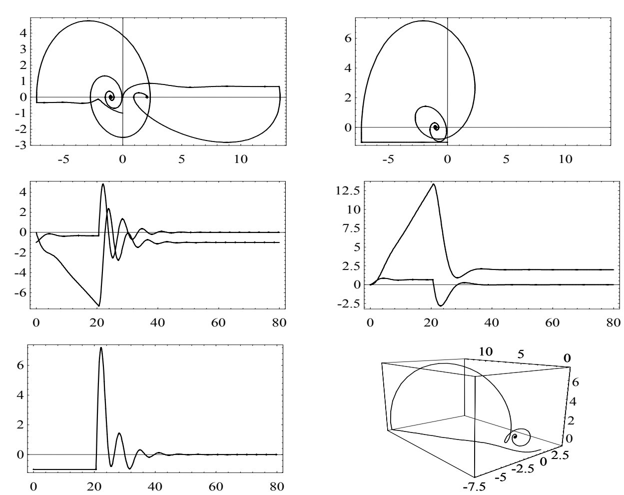

Fig. 14. $r = 0.5; \zeta = 2; s1 = 0.2; s2 = 0.3; fc1 = 1; fs1 = 7.4$
Fig.14[1,1]=Phase trajectories on the plane $\{\eta_1, \dot{\eta}_1\}$ and $\{\eta_2, \dot{\eta}_2\}$
Fig.14[1,2]=Phase trajectories on the plane $\{\eta_2, (\dot{\eta}_1 - \dot{\eta}_2)\}$
Fig.14[2,1]=Solution $\{\tau, \eta_1\}, \{\tau, \dot{\eta}_1\}$
Fig.14[2,2]=Solution $\{\tau, \eta_2\}, \{\tau, \dot{\eta}_2\}$
Fig.14[3,1]=Solution $\{\tau, \dot{\eta}_1 - \dot{\eta}_2\}$
Fig.14[3,2]=Solution $\{\eta_1, \eta_2, (\dot{\eta}_1 - \dot{\eta}_2)\}$

As it is deduced by the Figure 14, the fixed (for the integration) initial conditions are such that the phase trajectory run through the points of the space in which (25) is verified. In such way, the system dynamics will be influenced by the static friction and any limit cycles will be evident. The critical parameters sets, as it results from the Figure 14 [1,2], are those to which a phase trajectory that is tangent to

$$\dot{\eta}_1 - \dot{\eta}_2 = -1.$$

In Figure 15 the dynamic state evolution is brought as we have increased only the parameter f_{s1} value, point B of Figure 3b. The system, in this case, exhibits a limit cycle which slides vibrations correspond.

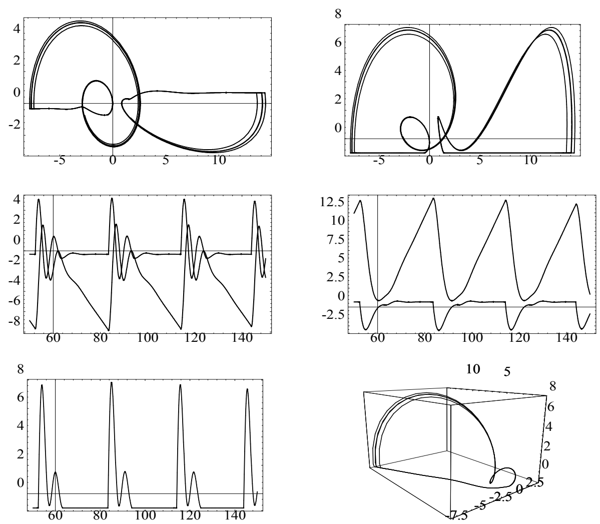

Fig. 15. $r = 0.5; \zeta = 2; s_1 = 0.2; s_2 = 0.3; f_{c1} = 1; f_{s1} = 7.8$
Fig.15[1,1]= Phase trajectories on the plane $\{\eta_1, \dot{\eta}_1\}$ and $\{\eta_2, \dot{\eta}_2\}$
Fig.15[1,2]=Phase trajectories on the plane $\{\eta_1, (\dot{\eta}_1 - \dot{\eta}_2)\}$ and $\{\eta_2, (\dot{\eta}_1 - \dot{\eta}_2)\}$
Fig.15[2,1]=Solution $\{\tau, \eta_1\}, \{\tau, \dot{\eta}_1\}$
Fig.15[2,2]=Solution $\{\tau, \eta_2\}, \{\tau, \dot{\eta}_2\}$
Fig.15[3,1]=Solution $\{\tau, \dot{\eta}_1 - \dot{\eta}_2\}$
Fig.15[3,2]=Solution $\{\eta_1, \eta_2, (\dot{\eta}_1 - \dot{\eta}_2)\}$

It could be shown that the stick phase, or the period interval in which there is no relative motion among the slides, increase when fs1 increase. In Figure 16 we have set $s_2 = 1.3$ (damping coefficient of the slide of mass m_2 greater than that "critical") and also in this case the system exhibits vibrations as shown in the same figure. Only when also the damping coefficient of the slide of mass m1 is greater than that "critical", then the system results "strongly" steady (absence of limit cycles).
In such case the trajectories degenerate in the equilibrium position without relative speed to be able in any case going to zero itself. It is opportune we observe that, for fixed rigidity and damping system values, the parameter f_{s1} grows when static friction increase and decreases when support speed increase.

IV. Conclusions

The proposed analysis makes it possible to assess the influence of the friction forces on the dynamic behavior of systems belonging to the class in question in order to establish their stability in the presence of self-excited (stick-slip) vibrations and, therefore, determine any slide positioning errors that may

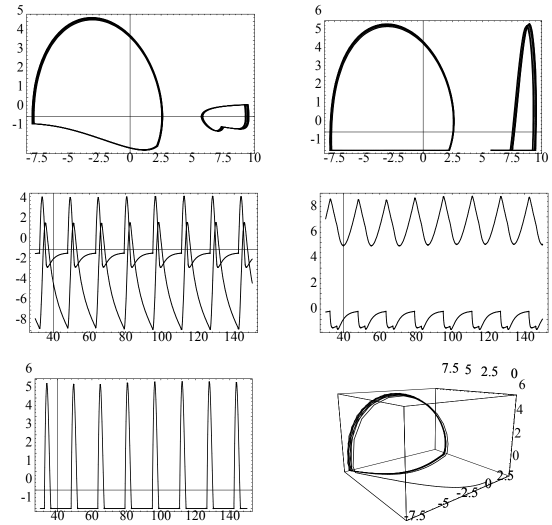

Fig. 16. $r = 0.5; \zeta = 2; s_1 = 1.3; s_2 = 0.3; f_{c1} = 1; f_{s1} = 7.4$
Fig. 16[1,1]= Phase trajectories on the plane $\{\eta_1, \dot{\eta}_1\}$ and $\{\eta_2, \dot{\eta}_2\}$
Fig. 16[1,2]=Phase trajectories on the plane $\{\eta_1, (\dot{\eta}_1 - \dot{\eta}_2)\}$and $\{\eta_2, (\dot{\eta}_1 - \dot{\eta}_2)\}$
Fig.16[2,1]=Solution $\{\tau, \eta_1\}, \{\tau, \dot{\eta}_1\}$
Fig.16[2,2]=Solution $\{\tau, \eta_2\}, \{\tau, \dot{\eta}_2\}$
Fig.16[3,1]=Solution $\{\tau, \dot{\eta}_1 - \dot{\eta}_2\}$
Fig.16[3,2]=Solution $\{\eta_1, \eta_2, (\dot{\eta}_1 - \dot{\eta}_2)\}$

occur in the drive mechanism stop phase.
In some conditions, the viscous damping and the variability of the friction force to the interface can affect normal system operation. The slide may stop late with respect to the drive mechanism and may thus cover more space and come to rest in a position different from the required and programmed one. The positioning error was determined by analyzing system evolution in the phases plane. The results obtained make it possible to predict slide positioning errors in the drive mechanism stop phase. An analysis of the diagrams in Figure 5 shows that the system in question is stable in stick-slip phenomena if the slope of the second section of the friction characteristic is greater than 1. Whereas, for slopes between 0 and 1 the system may display self-excited vibrations. Generally speaking, stick-slip instability arises with increases in the value of the difference E between static and kinetic friction in conditions of incipient motion and/or as the slope of the friction characteristic diminishes. On the other hand, positioning errors of the slide in Figure 1 can occur during the drive mechanism stop phase for a steep slope of the friction characteristic and/or low values of the E parameter. It is clear, therefore, that during design activity it is possible to eliminate positioning errors in the stop phase by making provision for viscous dampers with a suitable damping factor value. The en-suing slope variation of the friction characteristic must however be such as to avoid stick-slip instability phenomena. As it is always necessary to ensure a stable behavior in the presence of stick-slip phenomena but it is not always possible to avoid positioning errors, it is worthwhile here modifying the system parameters so as to minimize the positioning error. The present paper aims to give a conclusive synthesis of an initial stage of a research programme on "the dynamics of

tribomechanical systems". The subsequent phase will deal with modeling systems with more than one degree of freedom.

The dry friction influence upon the dynamic behavior of a two degrees of freedom mechanical system has been analyzed. From the system proposed results that:

1) The system can exhibit limit cycles for rigidity and damping values greater than critical one;
2) Vibrations occur if at least one of the parameters s_1 or s_2 is lower than one. Such vibrations can extinguish for finite perturbations of the dynamic state.

Being the parameter f_{s1} defined as the ratio between the static friction and the support speed, we can come to the conclusion that there are no vibrations when support speed increase and static friction decrease, respectively. Using the proposed method we will go on, in a next work, debugging the whole stability map in order to be able to foresee the vibrations onset, when the system parameters are known.

REFERENCES

[1] Roseau M., Vibrations in Mechanical Systems, Springer-Verlag, (1987).

[2] Capone G., D'Agostino V., Della Valle S., Guida D., Contributo allo studio delle vibrazioni autoeccitate indotte dall'attrito, La Meccanica Italiana, n. 222, 50-54, (1988).

[3] Capone G., D'Agostino V., Della Valle S., Guida D., Stick-slip Instability Analysis. Meccanica Vol. 27 n° 2, 111-118 (1992).

[4] Capone G., D'Agostino V., Della Valle S., Guida D., Friction-force characyteristic influence on positioning accuracy, Atti NORDTRIB '92 Vol. I, Helsinki 8-11 June 1992, 100-107.

[5] Capone G., D'Agostino V., Della Valle S., Guida D., Influence of the variation between static and kinetic friction on Stick-slip Instability, WEAR n° 161, 121-126 (1993).

[6] Capone G., D'Agostino V., Della Valle S., Guida D., Sulla dinamica di un sistema tribomeccanico a due gradi di libert, Atti Terzo Convegno AIMETA di Tribologia, Capri, 105-115 (1994).

[7] Capone G., D'Agostino V., Della Valle S., Guida D., Sulla dinamica di un sistema tribomeccanico a due gradi di libert, Atti Terzo Convegno AIMETA di Tribologia, Capri, 105-115 (1994).

[8] Capone G., D'Agostino V., Della Valle S., Guida D., Sull'instabilit indotta dall'attrito in sistemi a N gradi di libert, Atti XII Congresso Nazionale AIMETA, Napoli, 233, 238 (1995)

[9] S. D'Ambrosio, D. Guida, C. M. Pappalardo, J. Quartieri, Nonlinear Identification Method of Multibody System Parameters, *IPMM-2007 The 6th International Conference*, 1 (2007) 27-31.

[10] S. D'Ambrosio, C. Guarnaccia, D. Guida, T.L.L. Lenza, J. Quartieri, System Parameters Identification in a General Class of Non-linear Mechanical Systems, *International Journal of Mechanics*, 1 (2007) 76-79.

[11] D. Guida, J. Quartieri, S. Steri, A Procedure for Calculating an Approximate Analytical Response in a Large Class of Mechanical Systems, *WSEAS International Conference on Non-Linear Analysis*, Tenerife 2006.

[12] D. Guida, (2005), On the simulation of crankshaft dynamics. In: WSEAS SYSTEM SCIENCE and SIMULATION in ENGINEERING (ICOSSSE 2005). Tenerife (Spain), p. 12-16

[13] D. Guida, L. Durso (2005). Dry Friction Influence on Stability of a Mechanical System with Two Degree of Freedom. In: 7th WSEAS International Conference on Non-Linear Analysis, Non-Linear Systems and Chaose. Sofia, p. 56-60

[14] Guida D., Pappalardo C. M. (2009). Journal Bearing Parameter Identification. In: 11th WSEAS International Conference on Automatic Control, Modellig and Simulation. Istambul, May-30-June-01, p. 475-478

[15] Guida D., Pappalardo C. M. (2009). Sommerfeld and Mass Number Identification of Lubricated Journal Bearing. To be published on WSEAS Transaction.

[16] Brockley C.A., Cameron A., Potter A.F.,Friction-Induced Vibration,, Transaction of the A-SME-Journal of Lubrication technology, 101-108, (1967).

[17] Antoniou S.S., Cameron A., Gentle C.R.,The Friction Speed Relation from Stick-Slip Data, WEAR,36, 235-254, (1976).

[18] Capone G., D'Agostino V., della Valle S., Guida D., On the Self-excited Vibrations Due to Friction, La Meccanica Italiana, n 222, 50 - 54, (1988)

[19] Capone G., D'Agostino V., Della Valle S., Guida D., Stick-slip Instability Analysis. Meccanica,Vol. 27 n 2, 111-118 (1992).

[20] Capone G., D'Agostino V., Della Valle S., Guida D., Influence of the variation between static and kinetic friction on Stick-slip Instability, WEAR n 161, 121-126 (1993).

[21] Capone G., D'Agostino V., Della Valle S., Guida D., Friction-force characyteristic influence on positioning accuracy, NORDTRIB '92 Vol. I, Helsinki 8-11 June 1992, 100-107.

[22] Takano E., Hara T., Saeki M., Oscillations Caused by Solid Friction in a Hydraulic Driving System, JSME International Journal, Series III, Vol. 31, n. 1, 48-57, (1988).

[23] Gao C., Kuhlmann-Wilsdorf D., On Stick-slip and the Velocity Dependence of Friction at Low Speeds, ASME Journal of Tribology, Vol. 112, Apr. 354-360, (1990).

[24] Stoker J.J., Nonlinear Vibrations in Mechanical and Electrical Systems, New York, Interscience Publisher, (1950).

[25] Blaquiere A., Nonlinear System Analysis, New York and London, Academic Press, (1966).